

The impact of ageing on ¹¹C-Hydroxyephedrine uptake in the rat heart

Rudolf A. Werner, Xinyu Chen, Yoshifumi Maya, Christoph Eissler, Mitsuru Hirano, Naoko Nose, Hiroshi Wakabayashi, Constantin Lapa, Mehrbod S. Javadi, Takahiro Higuchi

Angaben zur Veröffentlichung / Publication details:

Werner, Rudolf A., Xinyu Chen, Yoshifumi Maya, Christoph Eissler, Mitsuru Hirano, Naoko Nose, Hiroshi Wakabayashi, Constantin Lapa, Mehrbod S. Javadi, and Takahiro Higuchi. 2018. "The impact of ageing on ¹¹C-Hydroxyephedrine uptake in the rat heart." *Scientific Reports* 8 (1): 8:11120.
<https://doi.org/10.1038/s41598-018-29509-0>.



SCIENTIFIC REPORTS



OPEN

The Impact of Ageing on ¹¹C-Hydroxyephedrine Uptake in the Rat Heart

Rudolf A. Werner^{1,2,3}, Xinyu Chen^{1,3}, Yoshifumi Maya⁴, Christoph Eissler¹, Mitsuru Hirano^{1,3}, Naoko Nose⁵, Hiroshi Wakabayashi^{1,3}, Constantin Lapa¹, Mehrbod S. Javadi² & Takahiro Higuchi^{1,3,5}

We aimed to explore the impact of ageing on ¹¹C-hydroxyephedrine (¹¹C-HED) uptake in the healthy rat heart in a longitudinal setting. To investigate a potential cold mass effect, the influence of specific activity on cardiac ¹¹C-HED uptake was evaluated: ¹¹C-HED was synthesized by N-methylation of (–)-metaraminol as the free base (radiochemical purity >95%) and a wide range of specific activities (0.2–141.9 GBq/μmol) were prepared. ¹¹C-HED (48.7 ± 9.7 MBq, ranged 0.2–60.4 μg/kg cold mass) was injected in healthy Wistar Rats. Dynamic 23-frame PET images were obtained over 30 min. Time activity curves were generated for the blood input function and myocardial tissue. Cardiac ¹¹C-HED retention index (%/min) was calculated as myocardial tissue activity at 20–30 min divided by the integral of the blood activity curves. Additionally, the impact of ageing on myocardial ¹¹C-HED uptake was investigated longitudinally by PET studies at different ages of healthy Wistar Rats. A dose-dependent reduction of cardiac ¹¹C-HED uptake was observed: The estimated retention index as a marker of norepinephrine function decreased at a lower specific activity (higher amount of cold mass). This observed high affinity of ¹¹C-HED to the neural norepinephrine transporter triggered a subsequent study: In a longitudinal setting, the ¹¹C-HED retention index decreased with increasing age. An age-related decline of cardiac sympathetic innervation could be demonstrated. The herein observed cold mass effect might increase in succeeding scans and therefore, ¹¹C-HED microPET studies should be planned with extreme caution if one single radiosynthesis is scheduled for multiple animals.

As the predominant disorder of the ageing population, heart failure (HF) is the major cause of death in both the United States and Europe^{1,2}. In this regard, HF can be understood as the result of cardiovascular ageing, representing the convergence of age-related alterations in both cardiovascular structure and function³.

Increasing interest in the age-dependent alterations in myocardial sympathetic nerve integrity has been aroused in particular from recognition that neurohumoral mechanisms may be the cause for the age-related increase in cardiovascular morbidity and mortality^{4–7}. Deterioration in cardiac innervation in the elderly population is characterized by an elevated plasma concentration of the neurotransmitter norepinephrine (NE)^{8,9}, an increased firing rate in the postganglionic fibers to the skeletal muscle^{10,11}, impaired function of the NE transporter (uptake-1 mechanism)^{4,5} and reduced plasma clearance of NE in the synaptic cleft^{12,13}.

The diagnostic use of cardiac radionuclide imaging probes such as ¹²³I-metaiodobenzylguanidine (¹²³I-mIBG) for Single Photon Emission Computed Tomography (SPECT) or ¹¹C-hydroxyephedrine (¹¹C-HED) for Positron Emission Tomography (PET) is currently expanding^{14–17}. Both radiotracers are considered to reflect sympathetic presynaptic function, as they share NE pathways and therefore interact with uptake-1 mechanism, which recovers exocytotically released NE from the synaptic cleft^{18–21}. An extensive body of evidence has been reported on the utility for risk stratification among severe HF patients using both imaging agents^{22–24}. In the prospective Prediction of Arrhythmic Events with Positron Emission Tomography (PAREPET)

¹Department of Nuclear Medicine, University of Würzburg, Würzburg, Germany. ²The Russell H. Morgan Department of Radiology and Radiological Science, Division of Nuclear Medicine and Molecular Imaging, Johns Hopkins University School of Medicine, Baltimore, MD, United States. ³Comprehensive Heart Failure Center (CHFC), University of Würzburg, Würzburg, Germany. ⁴Research Centre, Nihon Medi-Physics Co., Ltd., Chiba, Japan. ⁵Department of Biomedical Imaging, National Cerebral and Cardiovascular Center, Suita, Japan. Correspondence and requests for materials should be addressed to T.H. (email: thiguchi@me.com)

trial, sympathetic neuronal impairment assessed by ^{11}C -HED predicted sudden cardiac arrest independently of left ventricular ejection fraction²⁵. Apart from that, the impact of ageing on cardiac innervation assessed by ^{123}I -mIBG has also been reported previously, e.g. in healthy subjects^{26–29} or in patients suffering from systolic HF³⁰. Of note, Rengo *et al.* even suggested an age-dependent adjustment of the well-established ^{123}I -mIBG heart-to-mediastinum ratios, which are frequently used for stratifying the risk of cardiac events³⁰.

Hence, given the expected broadened use of ^{11}C -HED outside of controlled clinical trials as well as the alterations of myocardial sympathetic nerve function in the elderly, we aimed to explore the potential impact of ageing on cardiac ^{11}C -HED uptake in healthy rats in a longitudinal setting.

Materials and Methods

Animal protocols were approved by the local Animal Care and Use Committee (National Cardiovascular and Cerebral Research Center, Suita, Japan) and conducted according to the Guide for the Care and Use of Laboratory Animals (NIH Publication No. 85-23, revised 1996)³¹.

Study Design. The first study was performed to explore a potential cold mass effect on myocardial ^{11}C -HED uptake. Thereafter, the impact of ageing on cardiac ^{11}C -HED uptake was examined in a longitudinal setting.

Imaging Protocols. All animals were maintained under anesthesia throughout the imaging procedure with 2% isoflurane. ^{11}C -HED imaging was performed using a micro PET system (Inveon; Siemens Healthcare, Erlangen, Germany). Its characteristics have been described in³². Prior to a bolus tracer injection of ^{11}C -HED (50 MBq) via the tail vein, a list mode 30 min image acquisition was started. The list mode data was reconstructed into a dynamic sequence (23 frames: $15 \times 8\text{ s}$, $3 \times 60\text{ s}$, $5 \times 300\text{ s}$) using ordered-subset expectation maximization with 16 subsets and 4 iterations³³. For the second study (impact of ageing on myocardial ^{11}C -HED uptake), a reference scan with ^{18}F -fluorodeoxyglucose (^{18}F -FDG) was performed after more than four half lives of ^{11}C decay. One hour after i.v. administration of 37 MBq ^{18}F -FDG, PET images were acquired over 7 min. List-mode data were reconstructed using ordered-subset expectation maximization with 16 subsets and 4 iterations. The cardiac ^{18}F -FDG uptake was visualized as the percentage of the injected dose per tissue cubic ml (%ID/ml) and an imaging-processing application (AMIDE-bin 1.0.2) was used³⁴.

Effect of specific activity on myocardial ^{11}C -HED uptake. ^{11}C -HED was synthesized by N-methylation of (–)-metaraminol as the free base (radiochemical purity >95%) and a wide range of specific activities (0.2–141.9 GBq/ μmol) were prepared. Under isoflurane anesthesia, ^{11}C -HED ($48.7 \pm 9.7\text{ MBq}$, ranged 0.2–60.4 $\mu\text{g}/\text{kg}$ cold mass) was injected via the tail vein in 14 healthy female Wistar rats (Charles River Laboratories, 350–440 g) and dynamic PET images were obtained over 30 min. All animals received approximately the same mass dose of metaraminol ($1.5 \pm 1.4\mu\text{g}/\text{kg}$), the precursor of ^{11}C -HED.

Regions of Interest (ROI) were drawn at the mid-ventricular level in all 14 animals for assessment of uptake in myocardial tissue and at the left atrial cavity* for obtaining blood activity. Cardiac ^{11}C -HED retention index (%/min) was calculated as myocardial tissue activity at 20–30 min divided by the integral of the blood activity curves. The washout rate (%/min) was calculated as follows: $(\text{mean cardiac counts}_{7.5\text{min}} - \text{mean cardiac counts}_{27.5\text{min}}) / (\text{mean cardiac counts}_{7.5\text{min}} \times 100/20\text{ (min)})$. The effect of cold mass on the retention index was evaluated by fitting the data to a dose-response model with variable slope (Equation 1):

$$Y = \text{Bottom} + (\text{Top}-\text{Bottom}) / (1 + 10^{((\text{LogEC50}-X) \times \text{HillSlope})}), \quad (1)$$

where Y is the Retention index, X is the log of dose, and EC50 is the median effective concentration. Bottom value was estimated from the blood activity at 20–30 min.

The relationship between cold mass and washout rate was assessed by fitting the data to a Michaelis-Menten kinetics (Equation 2):

$$Y = (\text{rate}_{\text{max}} \times X) / (K_{\text{dis}} + X), \quad (2)$$

where Y is the washout rate, X is the dose, rate_{max} is the maximum rate of radioactivity loss, and K_{dis} is the half-saturation dose.

Impact of ageing on myocardial ^{11}C -HED uptake. Serial ^{11}C -HED PET imaging was conducted in 7 healthy male Wistar Rats (Charles River Laboratories) at different ages (month (M) 2, 5, 11 and 15). ^{11}C -HED was synthesized as previously described³⁵. Obtained specific radioactivity was 370–740 GBq/ μmol and radiochemical purity was >95%. ^{18}F -FDG was synthesized in an in-house cyclotron according to the manufacturer's instructions.

Statistical Analysis. All results are displayed as mean \pm standard deviation. Statistical analysis was performed using StatMate III (ATMS Co., Ltd., Tokyo, Japan). Statistical significance between the groups was determined by one-way ANOVA followed by post hoc Tukey multiple comparison analysis. A P-value of less than 0.05 was assumed to be statistically significant.

Results

***In-vivo* blocking study.** ^{11}C -HED dynamic PET with different tracer specific activities showed rapid blood clearance and clear delineation of the myocardium in all animals. A dose-dependent reduction of cardiac ^{11}C -HED uptake with different specific activities was observed (Fig. 1A, representative axial PET images): With a low dose of 0.2 $\mu\text{g}/\text{kg}$, uptake in the left ventricular myocardium could be clearly visualized, while a slight decrease could be observed at a dose of 1 $\mu\text{g}/\text{kg}$. A further notable decline could be observed with 10 $\mu\text{g}/\text{kg}$, while

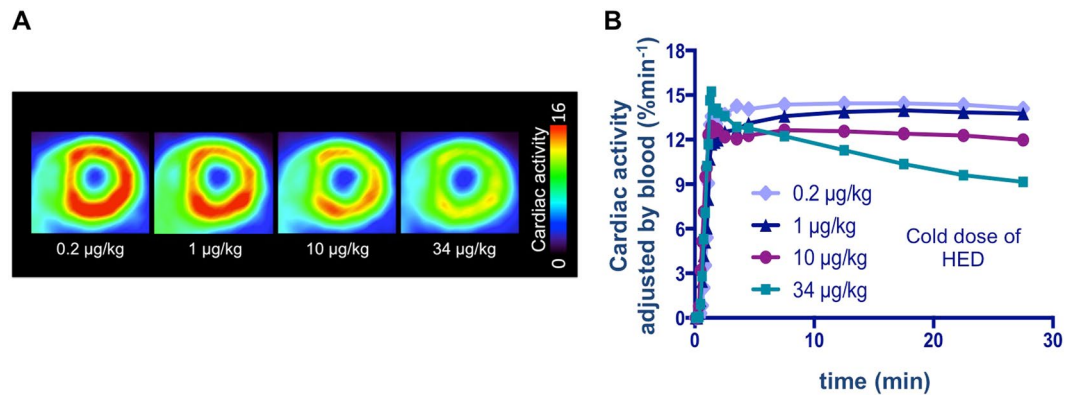


Figure 1. Uptake of radioactivity in the rat heart of 4 different animals (at an age of 2 months) after injection of ^{11}C -HED with different specific activities. **(A)** Representative axial PET images 25–30 min post-injection of ^{11}C -HED. **(B)** Time-activity curves for the myocardium with different amount of cold doses. A dose-dependent reduction of cardiac ^{11}C -HED uptake can be observed.

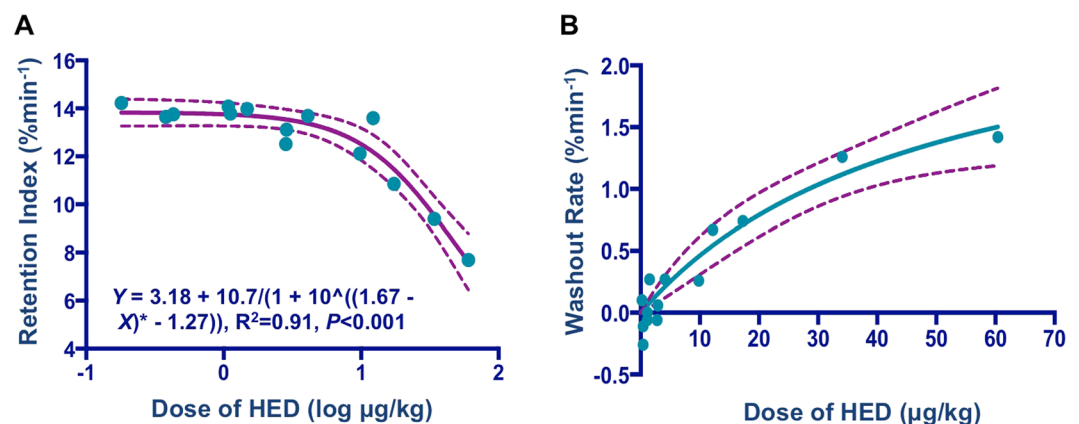


Figure 2. Dose-effect relationships for myocardial uptake of ^{11}C -HED. **(A)** Retention index. The estimated retention indices as a marker of norepinephrine re-uptake function decreased at lower specific activity (i.e. higher amount of cold mass). **(B)** Washout Rate. The washout rate increased as loaded cold mass increased. Every dot represents one investigated animal, dotted lines show 95% inclusion limits and solid lines indicate dose-effect curves.

myocardial uptake almost vanished with $34\ \mu\text{g}/\text{kg}$. Time-activity curves presented in Fig. 1B demonstrated that with the highest cold dose ($34\ \mu\text{g}/\text{kg}$), the washout considerably increased, while both the low-dose time-activity curves ($0.2\ \mu\text{g}/\text{kg}$ and $1\ \mu\text{g}/\text{kg}$) remained stable. The middle-dose time-activity curve ($10\ \mu\text{g}/\text{kg}$) demonstrated a moderate increase in washout.

The estimated retention index as a marker of norepinephrine re-uptake function decreased with lower specific activity (higher amount of cold mass, Fig. 2A). The data were well fitted by a dose-response model ($R^2 = 0.91$, $P < 0.001$) and the EC_{50} value (95% confidence intervals) was 46.3 (34.6 – 62) $\mu\text{g}/\text{kg}$. Notably, at a dose of $1\ \log\ \mu\text{g}/\text{kg}$, the retention index decreased at lower specific activity (Fig. 2A). Similar findings were also observed for the washout rate: at a cold dose of $10\ \mu\text{g}/\text{kg}$ HED, the washout rate increased markedly as loaded cold mass increased (Fig. 2B). The parameters calculated were $\text{rate}_{\text{max}} = 2.71\ \text{min}^{-1}$ and $K_{\text{dis}} = 48.7\ \mu\text{g}/\text{kg}$.

Longitudinal ^{11}C -HED imaging. In a longitudinal setting, serial ^{11}C -HED imaging was conducted at different ages of Wistar Rats. ^{11}C -HED PET images demonstrated clear visualization of the left ventricular wall indicating high and homogeneous tracer activity throughout the left ventricular myocardium for all animals at M2. However, the homogenous cardiac uptake pattern reduced subsequently from M5 to M11 and a further decline could be detected at M15. ^{18}F -FDG uptake remained stable throughout the ventricle at different ages, indicating preserved myocardial viability (Fig. 3A). ^{11}C -HED retention indices ($\%/ \text{min}$) decreased with increasing age (M2: 8.9 ± 2.2 , M5: 9.2 ± 1.09 , M11: 8 ± 1.64 , M15: 6.3 ± 1.1 ; M2 vs. M15, $p < 0.03$ and M5 vs. M15, $p < 0.02$, Fig. 3B).

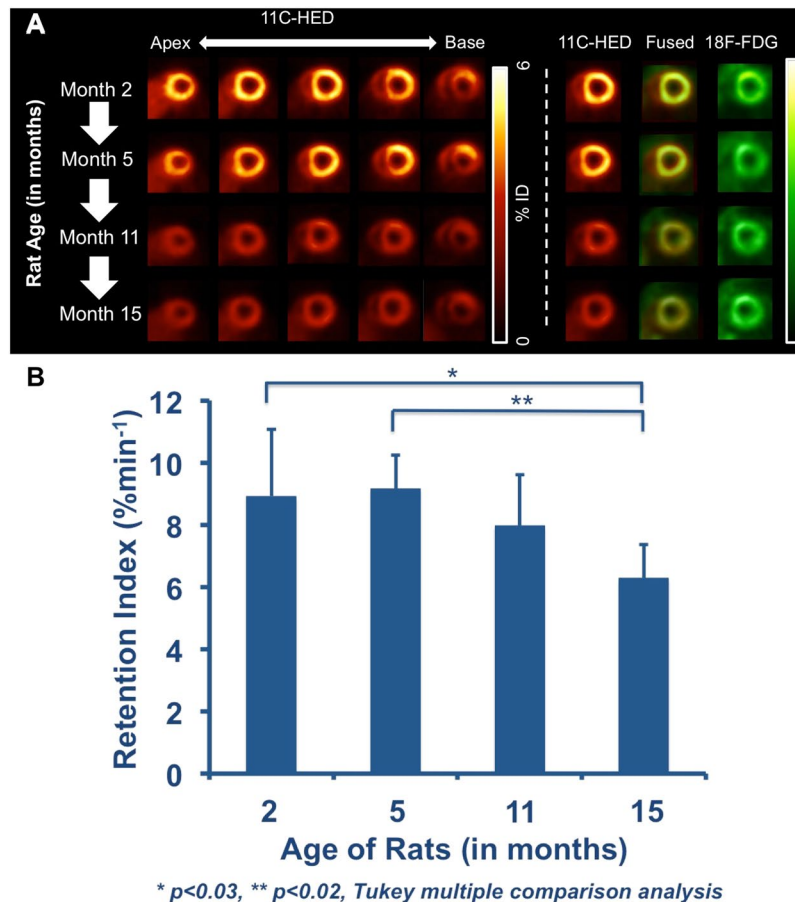


Figure 3. (A) *In-vivo* serial PET imaging with 11C-HED and 18F-FDG in healthy Wistar Rats at different ages (Month 2, 5, 11 and 15). An age-related decline of 11C-HED uptake can be observed, whereas 18F-FDG uptake remained stable at different ages. (B) Retention indices of rats at different ages (Month 2, 5, 11 and 15). Retention Indices decreased with increasing age (Month 2 and Month 5 vs. Month 15, $p < 0.03$ and $p < 0.02$, respectively).

Discussion

Cardiac sympathetic nerve PET tracers such as 11C-HED rely on the “uptake-1” recycling pathway^{18,19,36} and the present study demonstrated a high affinity of 11C-HED to the neuronal NE transporter: The estimated retention index as a marker of NE re-uptake function decreased at lower specific activity (i.e. higher amount of cold mass), while the washout rate increased. This observed effect triggered a subsequent investigation: The impact of ageing on 11C-HED uptake was investigated by a longitudinal imaging study in healthy rats and an age-related decline of cardiac sympathetic innervation could be demonstrated.

The high affinity of 11C-HED for neuronal uptake-1 has also been proven previously. However, species- and tracer-dependent variations have to be considered^{36,37}: In an *in-vivo* rabbit study, cardiac washout was enhanced by a desipramine chase protocol (i.e. addition of the uptake-1 blocker desipramine immediately after initial tracer accumulation), which suggests a continuous cyclical release (diffusion out) and reuptake of 11C-HED via neural NE transporter in the rabbit heart³³. Rischpler *et al.* investigated the same species like in the present study (Wistar Rats) and also demonstrated that desipramine led to a reduction of 11C-HED accumulation in the rat myocardium (while 123I-mIBG showed a high contribution to non-neuronal uptake-2)³⁷. DeGrado *et al.* further corroborated these observations by using 11C-HED in isolated perfused rat hearts³⁸. Hence, given the high affinity of 11C-HED to the neuronal NE transporter as demonstrated in the present study, the rat heart seems to serve as a suitable platform for 11C-HED sympathetic nerve imaging.

Considering the rapid radioactive decay of 11C labeled compounds (20.4 min) compared to 18F (110 min), lower specific activity (higher amount of cold mass) might hamper the diagnostic accuracy of 11C-HED studies. However, this problem can be neglected in a clinical setting, as normally one 11C-HED radiosynthesis is scheduled for one single patient injection. Nevertheless, the herein presented cold mass effect might be of utmost importance in planning small animal PET studies using 11C-HED^{39,40}: Analogous to patient care, only one radiotracer production should be considered for one animal, otherwise the cold mass might increase dramatically for the second, succeeding PET study. However, scanning one single animal per radiosynthesis might also lead to a significant cost expansion. Consequently, the findings of the present study should be at least taken into account if one 11C-HED radiosynthesis is scheduled for multiple animals. At a dose of 1 log $\mu\text{g}/\text{kg}$, the retention index decreased at lower specific activity (Fig. 2A). In a similar vein, at a cold dose of 10 $\mu\text{g}/\text{kg}$, the washout rate

increased markedly as loaded cold mass increased (Fig. 2B). Thus, those upper limits may serve as practical recommendations for conducting micro PET studies with 11C-HED.

An extensive body of evidence has reported on the general age-related changes in autonomic nervous system function^{41,42}. In particular, age-dependent alterations in myocardial sympathetic innervation have attracted interest because of the potential association between cardiac neurohumoral impairment and age-related increase in cardiovascular diseases^{4–7,43}. Apart from that, a more frequent use of the cardiac sympathetic nerve tracer 11C-HED can be envisaged in the near future, mainly due to its favourable properties for risk stratification among severe HF patients^{21,25}. Therefore, we also aimed to explore the impact of ageing on cardiac 11C-HED uptake in healthy Wistar rats and a decline of myocardial innervation with increasing age could be observed (Fig. 3). However, the concept of assessing an age-related effect on cardiac uptake-1 with neurohumoral PET or SPECT probes is not entirely novel: Tsuchimochi and coworkers demonstrated a decreasing inferior wall uptake in elder, healthy men using 123I-mIBG²⁷. In patients suffering from systolic HF, a paralleled decrease in both early and late heart-to-mediastinum ratios with increasing age has been reported³⁰. Li *et al.* investigated the F18-labelled neuronal imaging agent fluorodopamine in healthy volunteers and not surprisingly, an uptake reduction in the myocardium along with physiological human ageing could be observed⁴⁴. However, the investigation of a potential age-related impact among different cardiac sympathetic nerve tracers is of utmost importance, as all of these investigated PET or SPECT probes significantly differ in their kinetic properties (e.g., 11C-HED is resistant to degrading enzymes³⁶, whereas 6–18F-fluorodopamine shares similar metabolic pathways to physiological NE⁴⁴).

Of note, Bernacki *et al.* recently compared a younger patient cohort (18–33 y) vs. an older cohort (65–80 y) and reported on a decline in cardiac sympathetic nerve function assessed by 11C-HED PET. Although extrapolations from preclinical observations to humans must be done with extreme caution, the herein presented age-related decrease of sympathetic nerve function in the rat myocardium corroborates these previously reported findings⁴⁵. However, due to the preclinical setting of the present study, the same rat could be imaged at different time points of its life, which might be comparable to different stages in a human life cycle⁴⁶. M2 in a rat life corresponds approximately to early/middle childhood (human age, 6 y), M5 to adolescence (12–20 y), M11 to early adulthood/midlife (35–50 y) and M15 to mature adulthood (50–70 y). Hence, in contrast to Bernacki *et al.* selecting two extremes (adolescence vs. late adulthood)⁴⁵, the present study not only reports on significant differences in cardiac nerve function between young and old (M2 vs. M15 group), but also on an age-dependent loss of myocardial innervation over the life span of a healthy rat.

Conclusions

In a longitudinal 11C-HED imaging study in healthy rats, an age-related decline on myocardial sympathetic nerve activity could be demonstrated, which is consistent with the generalized decrease of peripheral somatic nerve function in the elderly. However, the herein reported cold mass effect might be of utmost importance in planning micro PET studies: only one production should be considered for one animal, as the cold mass might increase in succeeding scans for multiple animals.

References

- Lloyd-Jones, D. *et al.* Heart disease and stroke statistics—2009 update: a report from the American Heart Association Statistics Committee and Stroke Statistics Subcommittee. *Circulation* **119**, 480–486, <https://doi.org/10.1161/CIRCULATIONAHA.108.191259> (2009).
- Katsanos, S., Bistola, V. & Parissis, J. T. Acute Heart Failure Syndromes in the Elderly: The European Perspective. *Heart Fail Clin* **11**, 637–645, <https://doi.org/10.1016/j.hfc.2015.07.010> (2015).
- Strait, J. B. & Lakatta, E. G. Aging-associated cardiovascular changes and their relationship to heart failure. *Heart Fail Clin* **8**, 143–164, <https://doi.org/10.1016/j.hfc.2011.08.011> (2012).
- Esler, M. D. *et al.* Effects of aging on the responsiveness of the human cardiac sympathetic nerves to stressors. *Circulation* **91**, 351–358 (1995).
- Esler, M. D. *et al.* Aging effects on human sympathetic neuronal function. *Am J Physiol* **268**, R278–285, <https://doi.org/10.1152/ajpregu.1995.268.1.R278> (1995).
- Ferrari, A. U. Modifications of the cardiovascular system with aging. *Am J Geriatr Cardiol* **11**, 30–33 (2002).
- Davies, C. H., Ferrara, N. & Harding, S. E. Beta-adrenoceptor function changes with age of subject in myocytes from non-failing human ventricle. *Cardiovasc Res* **31**, 152–156 (1996).
- Fiorica, V. Plasma norepinephrine levels of elderly men on a controlled sodium intake diet. *J Am Geriatr Soc* **32**, 576–580 (1984).
- Veith, R. C., Featherstone, J. A., Linares, O. A. & Halter, J. B. Age differences in plasma norepinephrine kinetics in humans. *J Gerontol* **41**, 319–324 (1986).
- Matsukawa, T., Sugiyama, Y., Watanabe, T., Kobayashi, F. & Mano, T. Gender difference in age-related changes in muscle sympathetic nerve activity in healthy subjects. *Am J Physiol* **275**, R1600–1604 (1998).
- Yamada, Y., Miyajima, E., Tochikubo, O., Matsukawa, T. & Ishii, M. Age-related changes in muscle sympathetic nerve activity in essential hypertension. *Hypertension* **13**, 870–877 (1989).
- Esler, M. *et al.* Effects of aging on epinephrine secretion and regional release of epinephrine from the human heart. *J Clin Endocrinol Metab* **80**, 435–442, <https://doi.org/10.1210/jcem.80.2.7852502> (1995).
- Esler, M. *et al.* The influence of aging on the human sympathetic nervous system and brain norepinephrine turnover. *Am J Physiol Regul Integr Comp Physiol* **282**, R909–916, <https://doi.org/10.1152/ajpregu.00335.2001> (2002).
- Dilsizian, V. & Eckelman, W. C. Myocardial Blood Flow and Innervation Measures from a Single Scan: An Appealing Concept but a Challenging Paradigm. *J Nucl Med* **56**, 1645–1646, <https://doi.org/10.2967/jnumed.115.164251> (2015).
- Nakajima, K. & Nakata, T. Cardiac 123I-MIBG Imaging for Clinical Decision Making: 22-Year Experience in Japan. *J Nucl Med* **56**(Suppl 4), 11S–19S, <https://doi.org/10.2967/jnumed.114.142794> (2015).
- Henzlova, M. J., Duvall, W. L., Einstein, A. J., Travin, M. I. & Verberne, H. J. ASNC imaging guidelines for SPECT nuclear cardiology procedures: Stress, protocols, and tracers. *J Nucl Cardiol* **23**, 606–639, <https://doi.org/10.1007/s12350-015-0387-x> (2016).
- Rispler, S. *et al.* Quantitative 123I-MIBG SPECT/CT assessment of cardiac sympathetic innervation—a new diagnostic tool for heart failure. *Int J Cardiol* **168**, 1556–1558, <https://doi.org/10.1016/j.ijcard.2012.12.077> (2013).
- Thackeray, J. T. & Bengel, F. M. PET imaging of the autonomic nervous system. *Q J Nucl Med Mol Imaging* **60**, 362–382 (2016).
- Kobayashi, R. *et al.* New horizons in cardiac innervation imaging: introduction of novel (18)F-labeled PET tracers. *Eur J Nucl Med Mol Imaging* **44**, 2302–2309, <https://doi.org/10.1007/s00259-017-3828-8> (2017).

20. Chen, X. Y. *et al.* Radionuclide Imaging of Neurohormonal System of the Heart. *Theranostics* **5**, 545–558, <https://doi.org/10.7150/thno.10900> (2015).
21. Patel, H. C. *et al.* Targeting the autonomic nervous system: measuring autonomic function and novel devices for heart failure management. *Int J Cardiol* **170**, 107–117, <https://doi.org/10.1016/j.ijcard.2013.10.058> (2013).
22. Jacobson, A. F. *et al.* Myocardial iodine-123 meta-iodobenzylguanidine imaging and cardiac events in heart failure. Results of the prospective ADMIRE-HF (AdreView Myocardial Imaging for Risk Evaluation in Heart Failure) study. *J Am Coll Cardiol* **55**, 2212–2221, <https://doi.org/10.1016/j.jacc.2010.01.014> (2010).
23. Kasama, S., Toyama, T. & Kurabayashi, M. Serial (1)(2)(3)I-metaiodobenzylguanidine imaging predicts the risk of sudden cardiac death in patients with chronic heart failure. *Int J Cardiol* **179**, 82–83, <https://doi.org/10.1016/j.ijcard.2014.10.047> (2015).
24. Bengel, F. M. & Thackeray, J. T. Altered cardiac innervation predisposes to ventricular arrhythmia: targeted positron emission tomography identifies risk in ischemic cardiomyopathy. *J Am Coll Cardiol* **63**, 150–152, <https://doi.org/10.1016/j.jacc.2013.08.1629> (2014).
25. Fallavollita, J. A. *et al.* Regional Myocardial Sympathetic Denervation Predicts the Risk of Sudden Cardiac Arrest in Ischemic Cardiomyopathy. *Journal of the American College of Cardiology* **63**, 141–149, <https://doi.org/10.1016/j.jacc.2013.07.096> (2014).
26. Estorch, M., Carrio, I., Berna, L., Lopez-Pousa, J. & Torres, G. Myocardial iodine-labeled metaiodobenzylguanidine 123 uptake relates to age. *J Nucl Cardiol* **2**, 126–132 (1995).
27. Tschimochi, S. *et al.* Age and gender differences in normal myocardial adrenergic neuronal function evaluated by iodine-123-MIBG imaging. *J Nucl Med* **36**, 969–974 (1995).
28. Chen, W. *et al.* Age-related decrease in cardiopulmonary adrenergic neuronal function in children as assessed by I-123 metaiodobenzylguanidine imaging. *J Nucl Cardiol* **15**, 73–79, <https://doi.org/10.1016/j.nuclcard.2007.09.027> (2008).
29. Nakajima, K., Okuda, K., Matsuo, S., Wakabayashi, H. & Kinuya, S. Is (123)I-metaiodobenzylguanidine heart-to-mediastinum ratio dependent on age? From Japanese Society of Nuclear Medicine normal database. *Ann Nucl Med* **32**, 175–181, <https://doi.org/10.1007/s12149-018-1231-6> (2018).
30. Rengo, G. *et al.* Impact of aging on cardiac sympathetic innervation measured by (123)I-mIBG imaging in patients with systolic heart failure. *Eur J Nucl Med Mol Imaging* **43**, 2392–2400, <https://doi.org/10.1007/s00259-016-3432-3> (2016).
31. Bayne, K. Revised Guide for the Care and Use of Laboratory Animals available. American Physiological Society. *Physiologist* **39**(199), 208–111 (1996).
32. Disselhorst, J. A. *et al.* Image-quality assessment for several positron emitters using the NEMA NU 4-2008 standards in the Siemens Inveon small-animal PET scanner. *J Nucl Med* **51**, 610–617, <https://doi.org/10.2967/jnumed.109.068858> (2010).
33. Werner, R. A. *et al.* Retention Kinetics of the 18F-Labeled Sympathetic Nerve PET Tracer LM11195: Comparison with 11C-Hydroxyephedrine and 123I-MIBG. *Journal of nuclear medicine: official publication, Society of Nuclear Medicine* **56**, 1429–1433, <https://doi.org/10.2967/jnumed.115.158493> (2015).
34. Loening, A. M. & Gambhir, S. S. AMIDE: a free software tool for multimodality medical image analysis. *Mol Imaging* **2**, 131–137 (2003).
35. Rosenspire, K. C. *et al.* Synthesis and preliminary evaluation of carbon-11-meta-hydroxyephedrine: a false transmitter agent for heart neuronal imaging. *J Nucl Med* **31**, 1328–1334 (1990).
36. Chen, X. *et al.* Radionuclide imaging of neurohormonal system of the heart. *Theranostics* **5**, 545–558, <https://doi.org/10.7150/thno.10900> (2015).
37. Rischpler, C. *et al.* Discrepant uptake of the radiolabeled norepinephrine analogues hydroxyephedrine (HED) and metaiodobenzylguanidine (MIBG) in rat hearts. *Eur J Nucl Med Mol Imaging* **40**, 1077–1083, <https://doi.org/10.1007/s00259-013-2393-z> (2013).
38. DeGrado, T. R., Hutchins, G. D., Toorongian, S. A., Wieland, D. M. & Schwaiger, M. Myocardial kinetics of carbon-11-meta-hydroxyephedrine: retention mechanisms and effects of norepinephrine. *J Nucl Med* **34**, 1287–1293 (1993).
39. Thackeray, J. T. *et al.* Test-retest repeatability of quantitative cardiac 11C-meta-hydroxyephedrine measurements in rats by small animal positron emission tomography. *Nucl Med Biol* **40**, 676–681, <https://doi.org/10.1016/j.nucmedbio.2013.03.007> (2013).
40. Law, M. P. *et al.* Molecular imaging of cardiac sympathetic innervation by 11C-mHED and PET: from man to mouse? *J Nucl Med* **51**, 1269–1276, <https://doi.org/10.2967/jnumed.110.074997> (2010).
41. Pfeifer, M. A. *et al.* Differential changes of autonomic nervous system function with age in man. *Am J Med* **75**, 249–258 (1983).
42. Hotta, H. & Uchida, S. Aging of the autonomic nervous system and possible improvements in autonomic activity using somatic afferent stimulation. *Geriatr Gerontol Int* **10**(Suppl 1), S127–136, <https://doi.org/10.1111/j.1447-0594.2010.00592.x> (2010).
43. Nakou, E. S. *et al.* Healthy aging and myocardium: A complicated process with various effects in cardiac structure and physiology. *Int J Cardiol* **209**, 167–175, <https://doi.org/10.1016/j.ijcard.2016.02.039> (2016).
44. Li, S. T., Holmes, C., Kopin, I. J. & Goldstein, D. S. Aging-related changes in cardiac sympathetic function in humans, assessed by 6-18F-fluorodopamine PET scanning. *J Nucl Med* **44**, 1599–1603 (2003).
45. Bernacki, G. M. *et al.* Assessment of the Effects of Age, Gender, and Exercise Training on the Cardiac Sympathetic Nervous System Using Positron Emission Tomography Imaging. *J Gerontol A Biol Sci Med Sci* **71**, 1195–1201, <https://doi.org/10.1093/gerona/glw020> (2016).
46. Quinn, R. Comparing rat's to human's age: how old is my rat in people years? *Nutrition* **21**, 775–777, <https://doi.org/10.1016/j.nut.2005.04.002> (2005).

Acknowledgements

This work was supported by the Competence Network of Heart Failure funded by the Integrated Research and Treatment Center (IFB) of the Federal Ministry of Education and Research (BMBF) and German Research Council (DFG grant HI 1789/3-3). This project has received funding from the European Union's Horizon 2020 research and innovation programme under the Marie Skłodowska-Curie grant agreement No 701983. This publication was funded by the German Research Foundation (DFG) and the University of Wuerzburg in the funding programme Open Access Publishing.

Author Contributions

R.A.W., X.C., Y.M., H.W., C.L., T.H. designed the study, wrote the manuscript and researched data. R.A.W., X.C., Y.M., C.E., M.H., N.N., H.W. researched data, performed analysis and aided in drafting the manuscript. C.E., M.H., N.N., H.W. performed experiments and analyzed data. M.S.J. contributed to the discussion. C.L., M.S.J., T.H. designed the study, analyzed data and reviewed the manuscript.

Additional Information

Competing Interests: The authors declare no competing interests.

Publisher's note: Springer Nature remains neutral with regard to jurisdictional claims in published maps and institutional affiliations.



Open Access This article is licensed under a Creative Commons Attribution 4.0 International License, which permits use, sharing, adaptation, distribution and reproduction in any medium or format, as long as you give appropriate credit to the original author(s) and the source, provide a link to the Creative Commons license, and indicate if changes were made. The images or other third party material in this article are included in the article's Creative Commons license, unless indicated otherwise in a credit line to the material. If material is not included in the article's Creative Commons license and your intended use is not permitted by statutory regulation or exceeds the permitted use, you will need to obtain permission directly from the copyright holder. To view a copy of this license, visit <http://creativecommons.org/licenses/by/4.0/>.

© The Author(s) 2018